Correlations of Nearest-Neighbor Bonds at Short Times in the Internal Dynamics of Polyisobutylene

Donghwan Cho, Neal A. Neuburger, and Wayne L. Mattice*

Institute of Polymer Science, University of Akron, Akron, Ohio 44325-3909

Received May 7, 1991; Revised Manuscript Received September 10, 1991

ABSTRACT: A molecular dynamics trajectory of 1.8-ns duration has been computed for a methyl-terminated polyisobutylene, $C_{101}H_{204}$, at 400 K. Several time-averaged properties (mean-square end-to-end distance, averaged bond angles, and the numbers and locations of rotational isomeric states) deduced from the trajectory are in reasonable agreement with the results of earlier experiments and earlier theoretical investigations of the static properties of this polymer. The internal dynamics, on the time scale of the simulation, is dominated by $t^{\pm} \leftrightarrow t^{\mp}$ transitions, where t denotes trans. These transitions have a tendency to be correlated on a nearest-neighbor basis.

Introduction

The two pendant methyl groups bonded to alternate chain atoms in polyisobutylene produce steric crowding of short-range origin. Partial relief of this crowding is achieved by distortion of the $C-CH_2-C$ bond angles. This distortion is reflected in the results of experimental studies of the conformation of polyisobutylene in the solid state[1,2] and in the values used for the bond angles in theoretical studies,[3-6] as summarized in Table I. Our interest here is in the correlations in rotational isomeric state transitions in the short-time internal molecular dynamics of this crowded chain.

The initial focus will be on time-averaged conformation-dependent physical properties that can be extracted from the molecular dynamics trajectory. This section provides comparison with previous work insofar as the values of the bond angles, number and location of rotational states at the internal C–C bonds, and mean-square end-to-end distance are concerned. Then we will proceed to the analysis of the dynamics of the transitions between the rotational states, with emphasis on the fastest processes and their interdependence with events at neighboring bonds.

Method

The linear methyl-terminated polyisobutylene studied had the atomic composition $C_{101}H_{204}$. All hydrogen atoms were present discretely. The simulation was performed using CHARMm[7] as supplied by Polygen Corp.[8] All torsion angles, bond angles, and bond lengths were variable. Electrostatic contributions due to the Coulombic interaction of partial charges were ignored in the computation.

The emphasis will be on a trajectory for which the starting conformation was generated from the planar zigzag conformation by relaxation using a conjugate gradient method. Therefore, the starting conformation has an unusually high content of trans placements. The reason for this choice of starting conformation, and the implications, will be presented below. The classical Newton's equations of motion were integrated with a time step of 0.5 fs. The initial velocities were obtained from a Boltzmann distribution appropriate to the temperature. The temperature of the system, which is defined by the average kinetic energy of the atoms, was increased from 0 to 400 K and then equilibrated. After equilibration the temperature was computed every 500 fs. If the instantaneous temperature strayed more than ±10 K from the desired temperature, the velocities of all atoms were rescaled to maintain isothermal conditions. The trajectory at 400 K was computed for 1.8 ns, and the data were recorded at intervals of 100 fs.

In the analysis that summarizes the data as histograms depicting probabilities as a function of two consecutive dihedral angles, the bins used for collection of the data had an area of 5° × 5°.

Table I
Bond Angles (deg) in the Backbone of Polyisobutylene[a]

$C-CH_2-C$	CH_2-C-CH_2	ref
126	107	Bunn et al.[1]
128	110	Tanaka et al.[2]
124	110	Allegra et al.[3]
123	110	Boyd and Breitling[4]
124	110	Suter et al.[5,6]

[a] Experiment: refs 1 and 2. Calculations: ref 3–6.

Static Properties Deduced from the Trajectory

Characteristic Ratio. The end-to-end distance, r, fluctuated over a range of 4–48 Å during the trajectory, as depicted in Figure 1. The information in this figure can be compared with the characteristic ratio, C, defined as

$$C = \langle r^2 \rangle_0 / nl^2 \tag{1}$$

For this purpose, we simple average r^2 over the trajectory to obtain $\langle r^2 \rangle$, ignoring any correction for excluded volume. The implication of the replacement of $\langle r^2 \rangle$ for $\langle r^2 \rangle_0$ will be addressed in the next paragraph. The value of n is unambiguously defined as 50 by the covalent structure, and l will be identified with the mean length of a C–C bond, which is 1.53 Å. This approach yields

$$\langle r^2 \rangle / nl^2 = 5.8 \tag{2}$$

The value of C_∞, by which we mean the asymptotic limit for C as $n \rightarrow \infty$, has been determined from measurements of the intrinsic viscosity in two Θ solvents, benzene[9,10] and isovalerate.[11] The results are $6.6 \leq C_\infty \leq 6.9$ at 300 K. Using the values reported for the temperature coefficient, $d \ln \langle r^2 \rangle_0 / dT$,[12-15] the measurements at 300 K imply values in the range 6.3–6.9 at 400 K. The result obtained from the molecular dynamics trajectory, eq 2, is therefore about 10% smaller than the expectation for C_∞. Part of the difference can be attributed to the fact that eq 2 is based on the result obtained for a chain with $n = 50$. The effect of the finite number of bonds causes this chain to have a characteristic ratio slightly smaller than C_∞. The magnitude of this effect has been estimated by using the rotational isomeric state scheme described by DeBolt and Suter.[6] That scheme yields $C = 6.6$ as $n \rightarrow \infty$ and $C = 6.0$ at $n = 50$. The numerical value in eq 2 is only 3% smaller than the value computed for $n = 50$ from the rotational

0024-9297/92/2225-0322$03.00/0

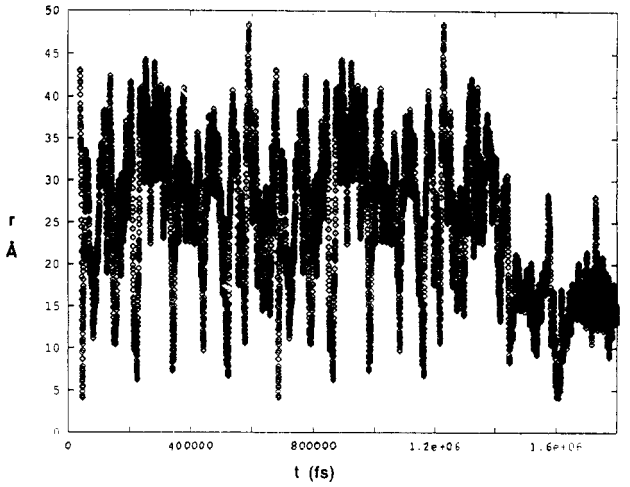

Figure 1. Instantaneous values of the end-to-end distance during the molecular dynamics trajectory at 400 K for a polyisobutylene with the composition $C_{101}H_{204}$.

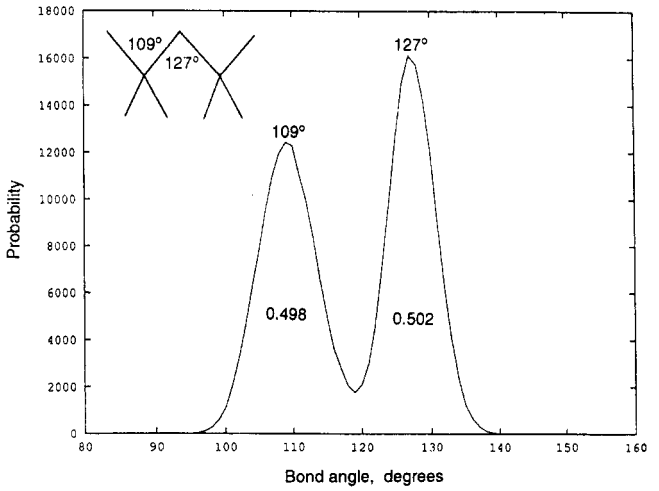

Figure 2. Probabilities for observation of values for the C–C–C bond angles in the main chain. The areas under the two peaks are in the ratio 0.498:0.502.

isomeric state approach. Since the molecular dynamics trajectory was computed in a vacuum, which acts as a poor solvent for polyisobutylene, one expects $\langle r^2 \rangle$ should be slightly smaller than $\langle r^2 \rangle_0$. We conclude that the result obtained from the simulation, eq 2, is reasonable, even though the chain has more t placements than expected for the unperturbed chain, as will be described below.

Bond Angles. Figure 2 depicts the distribution for the C–C–C bond angles in the main chain. The distribution shows two peaks, with maxima at 109° and 127°. The former peak, which is the CH_2–C–CH_2 bond angle, is somewhat broader than the latter peak, which is the C–CH_2–C bond angle. The breadth of the two peaks is sufficient to produce a weak overlap, with the probability passing through a minimum at 119°. Nearly identical areas (in the ratio 0.498:0.502) are enclosed in the distributions on either side of 119°.

The observation in the simulation that the CH_2–C–CH_2 bond angle prefers a value very close to the tetrahedral angle is in harmony with previous experimental and theoretical work, as summarized in Table I. The peak in Figure 2 for the C–CH_2–C bond angle is in excellent agreement with the experimental results[1,2] presented in Table I. It is a few degrees larger than the values of 123–124° used in previous theoretical work,[3-6] but the values fall well within the region of high probability for this bond angle in the simulations.

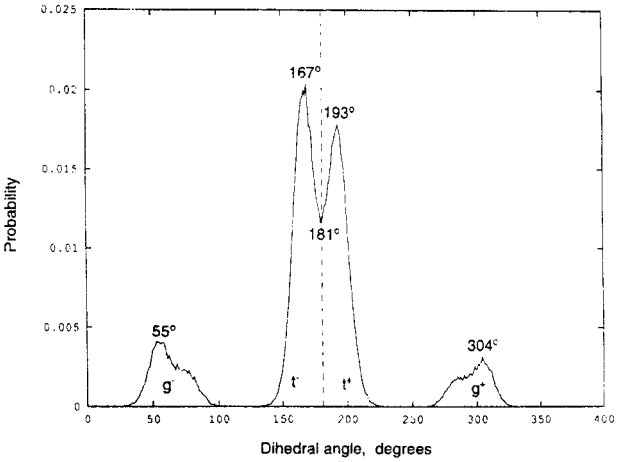

Figure 3. Probabilities for observation of different dihedral angles at C–C bonds in the main chain.

Dihedral Angles. Figure 3 depicts the probability distribution for the dihedral angle at an arbitrarily selected internal C–C bond in the main chain. The shape of the rotation potential demands that the true probability distribution should be symmetric about 0° and 180°. Minor departures from the anticipated symmetry are observed in Figure 3 because of the finite length of the trajectory. The probability distribution reveals discrete rotational isomers in the vicinity of 180° and 180 ± 120°. Each of these three rotational isomers is split into two peaks. This splitting is most readily apparent in the region near 180°, where the maxima occur at 180 ± 13°. These two peaks will be denoted t^- and t^+. The splitting of the gauche regions does not produce well-differentiated maxima but instead causes a pronounced shoulder on the side of the gauche peak that is in the direction of the trans state. Six states arise from the splitting of t, g^+, and g^-. The occurrence of these six states was first described by Boyd and Breitling.[4] Six states were also deduced from conformational energy calculations of dimeric through hexameric segments of polyisobutylene.[5,6] Suter et al. reduced the number of states to four, because the minor member of the pair in each gauche region was of negligible importance. They assigned dihedral angles of 180 ± 25° to the t^+ and t^- states and ±60° to the two gauche states. The results depicted in Figure 3 suggest that it might be reasonable to ignore the splitting of the gauche states. They also find a somewhat smaller splitting of t^+ and t^- than was used by Suter et al.

The distribution of dihedral angles depicted in Figure 3 differs from the distribution deduced previously from minimizations of the conformational energy of smaller oligomers[4-6] in that Figure 3 shows the $t^\pm$ states are more strongly occupied than the $g^\pm$ states. The rotational isomeric state model described by DeBolt and Suter[6] would yield equal populations for t^+, t^-, g^+, and g^-. Our result has a large population of $t^\pm$ states because nearly all internal bonds in the starting conformation are in $t^\pm$ states, and the time scale of the simulation does not permit a complete equilibration between the $t^\pm$ states and the $g^\pm$ states. The justification for this selection of a starting conformation is that our primary interest will be in $t^+ \leftrightarrow t^-$ transitions. We will not address the dynamics of the $t^\pm \leftrightarrow g^\pm$ transitions, except to point out they they occur on time scales that are much longer than those of the $t^+ \leftrightarrow t^-$ transition and longer than the time scale of the simulation.

Figure 4 depicts the interdependence of the dihedral angles. Here the probabilities are depicted as functions

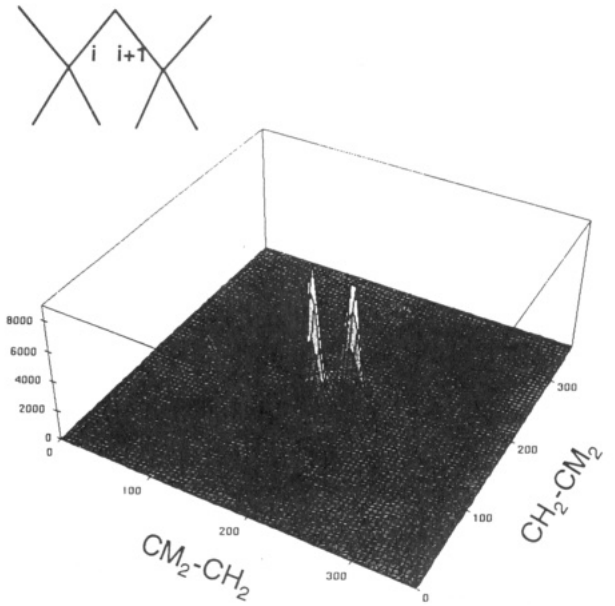

Figure 4. Probabilities for observation of pairs of dihedral angles at the two C–C bonds of a methyl group in the main chain.

of the two consecutive dihedral angles at bonds centered on a methylene group in the backbone. The splitting of the tt and tg peaks is readily apparent. Probabilities in the gg regions are too small to be easily recognized in Figure 4.

The central region of Figure 4 shows that there is a higher probability for successive trans states of the same sign (t^+t^+ or t^-t^-) than for successive trans placements of opposite sign (t^+t^- or t^-t^+). This feature is also seen in the rotational isomeric state model of DeBolt and Suter[6] for CH_2–C–CH_2. Our ready observations of it at the pair of bonds centered on CH_2 is facilitated by the choice of starting conformation for the trajectory, as described above in conjunction with the population of $t^\pm$ vs $g^\pm$. The correlated rotations away from ϕ_i, ϕ_{i+1} = 180°, 180° partially relieve the repulsions of the pendant methyl groups. The origin of this effect can be seen in a molecule as simple as *n*-pentane, where it causes the appearance of two distinct minima in the conformational energy surface in the regions where the internal C–C bonds adopt gauche placements of opposite sign.[16] If the boundary between t^+ and t^- in polyisobutylene is located precisely at the position where the value of ϕ is 180°, the probability for $t^\pm t^\mp$ is only 16–19% of the probability for $t^\pm t^\pm$. The most direct route for the coupled transition $t^\pm t^\pm \leftrightarrow t^\mp t^\mp$ can follow a path along which the probability is always recognizably higher than zero, on the scale used in the presentation of Figure 4.

Internal Dynamics Deduced from the Trajectory

The instantaneous conformation of the chain will be represented as a string of 48 symbols, one for each of the internal C–C bonds. The symbols are selected from +, −, p, and m, for t^+, t^-, g^+, and g^-, respectively. Figure 5 depicts the evolution of the conformation over 1.75 ns, with the record being written at intervals of 0.05 ns. This figure shows no direct transitions of the type $g^\pm \leftrightarrow g^\mp$ and only 18 transitions of the type $t \leftrightarrow g^\pm$. According to the sampling depicted in Figure 5, only 10 of the 48 internal C–C bonds visit both a t and g state during 1.75 ns. Most of the bonds (34) remain in the trans region throughout the trajectory, and four bonds remain in one of the gauche states. If the internal dynamics were to be equated to $t \leftrightarrow g^\pm$ isomerization, one would conclude that the chain was relatively

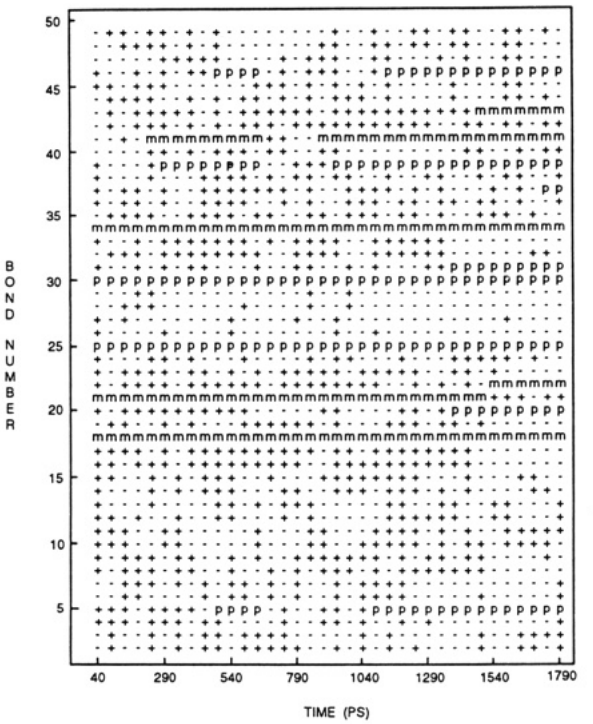

Figure 5. Instantaneous conformations of the chain, at intervals of 0.05 ns, over a 1.75-ns trajectory at 400 K. The states of the internal C–C bonds are denoted by +, −, p, and m for t^+, t^-, g^+, and g^-, respectively.

quiescent and that a much longer trajectory is required for analysis of the dynamics. Such a definition of internal dynamics is unnecessarily restrictive, because the end-to-end distance experiences more frequent fluctuations (see Figure 1) than can be accounted for by a mere 18 $t \leftrightarrow g^\pm$ transitions. Interest is therefore directed to the $t^\pm \leftrightarrow t^\mp$ transitions, which are much more frequent than the $t \leftrightarrow g^\pm$ transitions. They occur on a time scale that is shorter than the trajectory of 1.75 ns.

Figure 6 depicts an expansion of a 35-ps portion of the trajectory that was shown in Figure 5. On this time scale, no $t \leftrightarrow g^\pm$ transitions are observed, but there are numerous $t^\pm \leftrightarrow t^\mp$ transitions. A further expansion of the time scale is presented in Figure 7. One qualitative conclusion extracted from these figures is that the occurrence of t^+ and t^- is not random. Instead they tend to occur as strings with placements of the same sign. Another conclusion is that the lifetime of a t^+ or t^- state seems to depend on the states of its neighbors. The shortest lifetimes are seen for the middle state in the triplets $t^\pm t^\mp t^\pm$.

Quantitative evaluation of the lifetimes is presented in Figure 8. The decays cannot be described by a single exponential, and the deviation from a single exponential is greatest for the fastest decays, as shown in Figure 9. Clearly the lifetime of a $t^\pm$ state in the middle of a ttt sequence depends on the state of its neighbors. Average lifetimes, evaluated from the time dependence of the conditional probabilities, are presented in Table II. They vary by a factor of 3. The fact that the average lifetime increases when neighbors occupy t states of the same sign, and decreases when they occupy t states of the opposite sign, is easily rationalized by the positions of the two peaks in the probability profile in the tt region in Figure 4. The $t^\pm t^\pm$ junctions are more stable than the $t^\pm t^\mp$ junctions.

An instructive (although somewhat oversimplified) picture of the local internal dynamics emerges from Figures 5–8. At 400 K, the subnanosecond dynamics is dominated by the $t^\pm \leftrightarrow t^\mp$ transitions. Some of these transitions occur

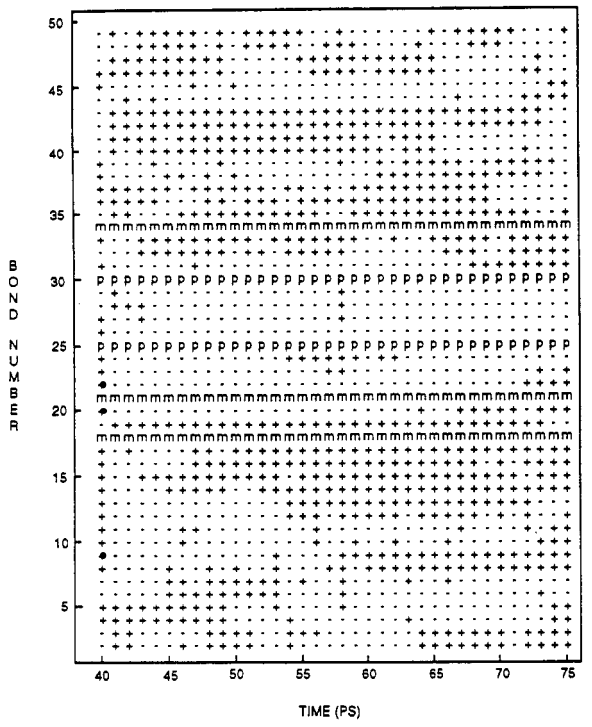

Figure 6. Instantaneous conformations at intervals of 1 ps, over a trajectory of 35 ps at 400 K.

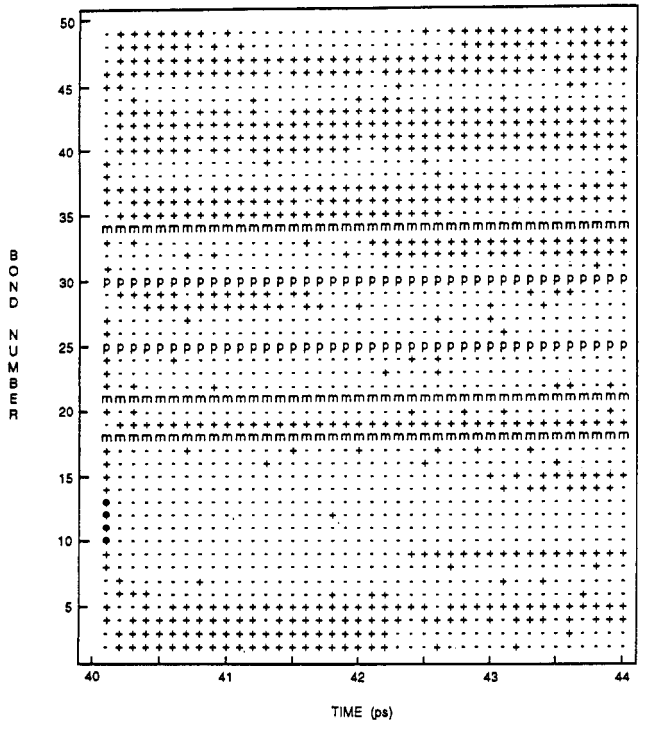

Figure 7. Instantaneous conformations at intervals of 0.1 ps, over a trajectory of 4 ps at 400 K.

at the junctions in sequences of the type ...$t^{\pm}t^{\mp}$... and therefore amount to migration of the $t^{\pm}t^{\mp}$ junction by a random walk in one dimension. This migration of the junction can eventually produce transitions at bonds that were initially in the middle of a sequence of t placements of the same sign. To the extent that this simple model is followed, there is a nearest-neighbor correlation in the transitions. This simple picture is not adhered to rigorously, because there are also occasional transitions, such as $t^{\pm}t^{\pm}t^{\pm} \rightarrow t^{\pm}t^{\mp}t^{\pm}$, that create new junctions. Most of these transitions are rapidly reversed, due to the very short lifetime of a t placement for which both neighbors are of opposite sign. The influence of these occasional transitions is sufficiently important so that the decay profiles do not adhere to the model described by Hall and Helfand, which combined an intrinsic rate of $+ \leftrightarrow -$ transitions with a rate for diffusion of the $+ -$ junction.[17] The dynamics of the $t \leftrightarrow g$ isomerization does not become important until the nanosecond time scale.

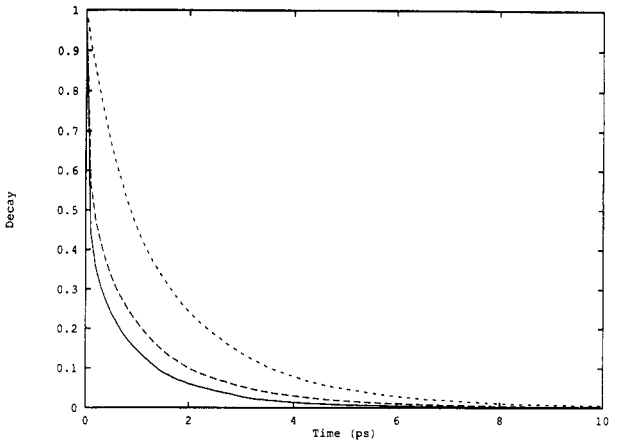

Figure 8. Conditional probability at 400 K that a bond in either the t^+ or t^- state at time zero, and with t states as nearest neighbors at that time, will remain continuously in the same state to time t. The three curves differentiate the bonds with respect to the states of their nearest neighbors at zero time. Short dashes: $t^{\pm}t^{\pm}t^{\pm}$. Long dashes: $t^{\pm}t^{\pm}t^{\mp}$ or $t^{\pm}t^{\mp}t^{\mp}$. Solid curve: $t^{\pm}t^{\mp}t^{\pm}$.

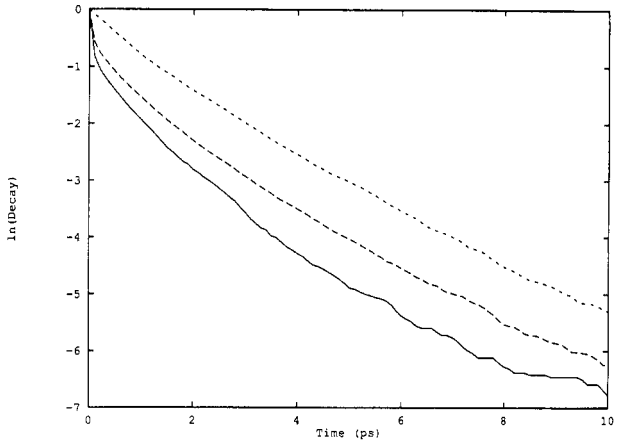

Figure 9. Semilogarithmic plot of the decays in Figure 8.

Table II
Average Lifetimes at 400 K for the t State in the Middle of a ttt Sequence

sequence at zero time	average lifetime, ps	sequence at zero time	average lifetime, ps
$t^{\pm}t^{\mp}t^{\pm}$	0.53	$t^{\pm}t^{\pm}t^{\pm}$	1.52
$t^{\pm}t^{\pm}t^{\mp}$, $t^{\pm}t^{\mp}t^{\mp}$	0.76		

The nearest-neighbor correlation in the rates of rotational isomeric state transitions is not confined to polyisobutylene. It is observed in the poly(dialkylsiloxanes) and is especially dramatic in poly(di-*tert*-butylsiloxane).[18]

Acknowledgment. This research was supported by National Science Foundation Grant DMR 89-15025.

References and Notes

(1) Bunn, C. W.; Holmes, D. R. *Faraday Discuss. Chem. Soc.* **1958**, *25*, 95.
(2) Tanaka, T.; Chantani, Y.; Tadokoro, H. *J. Polym. Sci., Polym. Phys. Ed.* **1974**, *12*, 515.
(3) Allegra, G.; Benedetti, E.; Pedone, C. *Macromolecules* **1970**, *3*, 727.

(4) Boyd, R. H.; Breitling, S. M. *Macromolecules* **1972**, *5*, 1.
(5) Suter, U. W.; Saiz, E.; Flory, P. J. *Macromolecules* **1983**, *16*, 1317.
(6) DeBolt, L. C.; Suter, U. W. *Macromolecules* **1987**, *20*, 1425.
(7) Brooks, B. R.; Bruccoleri, R. E.; Olafson, B. D.; States, D. J.; Swaminathan, S.; Karplus, M. *J. Comput. Chem.* **1983**, *4*, 187.
(8) Polygen Corporation, 200 Fifth Avenue, Waltham, MA 02254.
(9) Fox, T. G., Jr.; Flory, P. J. *J. Am. Chem. Soc.* **1951**, *73*, 1909.
(10) Krigbaum, W. R.; Flory, P. J. *J. Polym. Sci.* **1953**, *9*, 37.
(11) Matsumoto, T.; Nishioka, N.; Fujita, H. *J. Polym. Sci., Polym. Phys. Ed.* **1972**, *10*, 23.
(12) Ciferri, A.; Hoeve, C. A. J.; Flory, P. J. *J. Am. Chem. Soc.* **1961**, *83*, 1015.
(13) Chiang, R. *J. Phys. Chem.* **1966**, *70*, 2348.
(14) Mark, J. E.; Thomas, G. B. *J. Phys. Chem.* **1966**, *70*, 3588.
(15) Allen, G.; Gee, G.; Kirkham, M. C.; Price, C.; Padget, J. *J. Polym. Sci.* **1968**, *23*, 201.
(16) Abe, A.; Jernigan, R. L.; Flory, P. J. *J. Am. Chem. Soc.* **1966**, *88*, 631.
(17) Hall, C. K.; Helfand, E. *J. Chem. Phys.* **1982**, *77*, 3275.
(18) Neuburger, N. A.; Mattice, W. L. *Polym. Prepr. (Am. Chem. Soc., Div. Polym. Chem.)* **1991**, *32* (2), 279.